



ORIGINAL ARTICLE

Application of asymmetric dicationic ionic liquids for oil spill remediation in sea water



C.E. El shafiee ^a, R.A. El-Nagar ^{a,*}, M.I. Nessim ^a, M.M.H. Khalil ^b, M.E. Shaban ^b, Rima D. Alharthy ^c, D.A Ismail ^a, R.I. Abdallah ^a, Y.M. Moustafa ^a

^a Egyptian Petroleum Research Institute, Egypt

^b Ain Shams University, Egypt

^c King Abdulaziz University, KSA

Received 14 January 2021; accepted 14 March 2021

Available online 24 March 2021

KEYWORDS

Ionic liquids;
Amphiphilic;
Imidazoles;
Oil spill dispersants;
Surface tension;
UV

Abstract Three asymmetric dicationic ionic liquids; 1-(2-(1-dodecyl-2-methyl-1*H*-imidazol-3-ium-3-yl)ethyl)-4-methylpyridin-1-ium bromide, 1-(6-(1-dodecyl-2-methyl-1*H*-imidazol-3-ium-3-yl)hexyl)-4-methylpyridin-1-ium bromide and 1-(10-(1-dodecyl-2-methyl-1*H*-imidazol-3-ium-3-yl) decyl)-4-methylpyridin-1-ium bromide (Ia, Ib & Ic respectively) were synthesized and characterized via Elemental analysis, FT-IR, ¹H NMR, and Thermo-gravimetric analysis (TGA). Their surface activities were studied. The performance of the synthesized ionic liquids as oil spill dispersants were evaluated at different temperatures (10, 30 & 50 °C) and concentrations (750, 1500, 2000, 3000 ppm). Data reveals that the efficiency is ranked as follows: Ib > Ia > Ic with concentration of 1500 ppm.

© 2021 The Author(s). Published by Elsevier B.V. on behalf of King Saud University. This is an open access article under the CC BY-NC-ND license (<http://creativecommons.org/licenses/by-nc-nd/4.0/>).

1. Introduction

Through the world wide fast development of marine transportation and oil exploration, the oil spills became the major contributors to the marine pollution and cause many environmental catastrophes (Huang et al., 2019; Naser, 2013). Oil spills may result from the rupture of pipeline and holding tanks or well blowout (Komoto and Kobayashi, 2004). Oil

spills would float and spread on water due to the smaller gravity and surface energy so, the marine ecosystem remarkably contaminated and the algae primary production decreased because of depletion of light into the water (Penela-Arenaz et al., 2009).

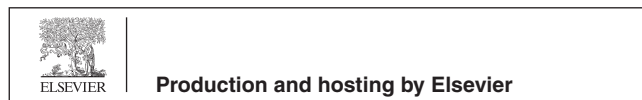
The methods of oil spill treatment in aquatic environment have different classifications mechanical, biological and chemical techniques (Muhd Julkapli et al., 2011). In mechanical method engineers using skimmers, oil booms, barriers or sorbents and need different instruments to physically absorb or suck up oil from water surface. In biological method micro-organisms could eat or break down the toxic components or oil spill into nontoxic materials but this way of remediation is slow and not adapted in cold areas (Behera and Ray, 2016).

In chemical treatment the dispersion mechanism is to minimize the oil droplets size by reducing the interfacial tension

* Corresponding author.

E-mail address: raghda_elnagar@yahoo.com (R.A. El-Nagar).

Peer review under responsibility of King Saud University.



between oil and water under the effect of wave action as the smaller droplets, the more dispersion efficiency (Kujawinski et al., 2011). The usage of chemical dispersants in marine environment is worldwide accepted; however, most of them are toxic and hazardous to the marine habitats. From this point ionic liquids received highly attention because of their technological and environmental promising (Adeniyi Ogunlaja et al., 2018) benefits (low toxicity (Visser et al., 2011), low volatility (Li et al., 2008; Ezzat et al., 2018; Atta et al., 2018; Atta et al., 2017; Abdullah et al., 2017), high surface activity and thermal stability) (Pandey, 2006; Wilkes, 2002; Li et al., 2009) furthermore the self-assembling properties of amphiphilic ionic liquids (Adawiyah et al., 2019; Lotfi et al., 2017; El-Nagar et al., 2017).

In this work three amphiphilic asymmetric dicationic ionic liquids (green compounds) were successfully synthesized and characterized (Table 1). The synthesized series possess high surface activity and evaluated as oil spill dispersants.

2. Experimental

2.1. Materials and methodology

- All chemicals and reagents were purchased from international chemical companies. They are of analytical grade and used directly without further purification. 1-bromododecane (98%), 2-methyl imidazole (99%) and potassium hydroxide (97%), Sigma-Aldrich. 4-Methyl pyridine (99%), acetonitrile (97%), 1,2-dibromoethane (99%), 1,6-dibromohexane (99%), 1,10-dibromodecane (99%), and ethyl acetate (98%) Merck. Petroleum ether (40–60) (98%), aluminium hydroxide (neutral), filter paper Whatman No.1 and chloroform (99%), Alfa Aesar. Sea water (Red Sea) and heavy crude oil from Suez Golf.
- Synthesis of dicationic ionic liquids (Ia – c):**

The mechanisms of synthesis were illustrated as follows:

- (i) Compound (I) was prepared before (El-Taib Heakal et al., 2017) by stirring 2-methyl imidazole (0.1 mol) with potassium hydroxide in acetonitrile (50 ml). After complete miscibility 1-bromododecane (0.1 mol) was added

drop wise, the stirring completed till white precipitate was formed (about 3hrs). White precipitate (KBr) was eliminated by filtration and the filtrate vaporized under vacuum.

- (ii) Compounds [a, b and c] were prepared by stirring 4-methyl pyridine (0.1 mol) with n-di-bromo alkanes (0.1 mol) (1,2-dibromoethane, 1,6-dibromohexane and 1,10-dibromodecane) at room temperature for 3hrs. The products were washed several times with ethyl acetate to get rid of unreacted materials. White precipitate was afforded by filtration and recrystallized from petroleum ether 40–60 (Chang et al., 2010).
- (iii) Ia, Ib and Ic dicationic ionic liquids were synthesized by refluxing mixtures of compound I with a, b and c, (1:1), for 3 hrs in presence of acetonitrile as a solvent. The mixtures were concentrated by evaporation of acetonitrile and dried under vacuum (Lv et al., 2019) Scheme 1.

2.2. Characterization

The chemical structures of (Ia – c) were confirmed via.

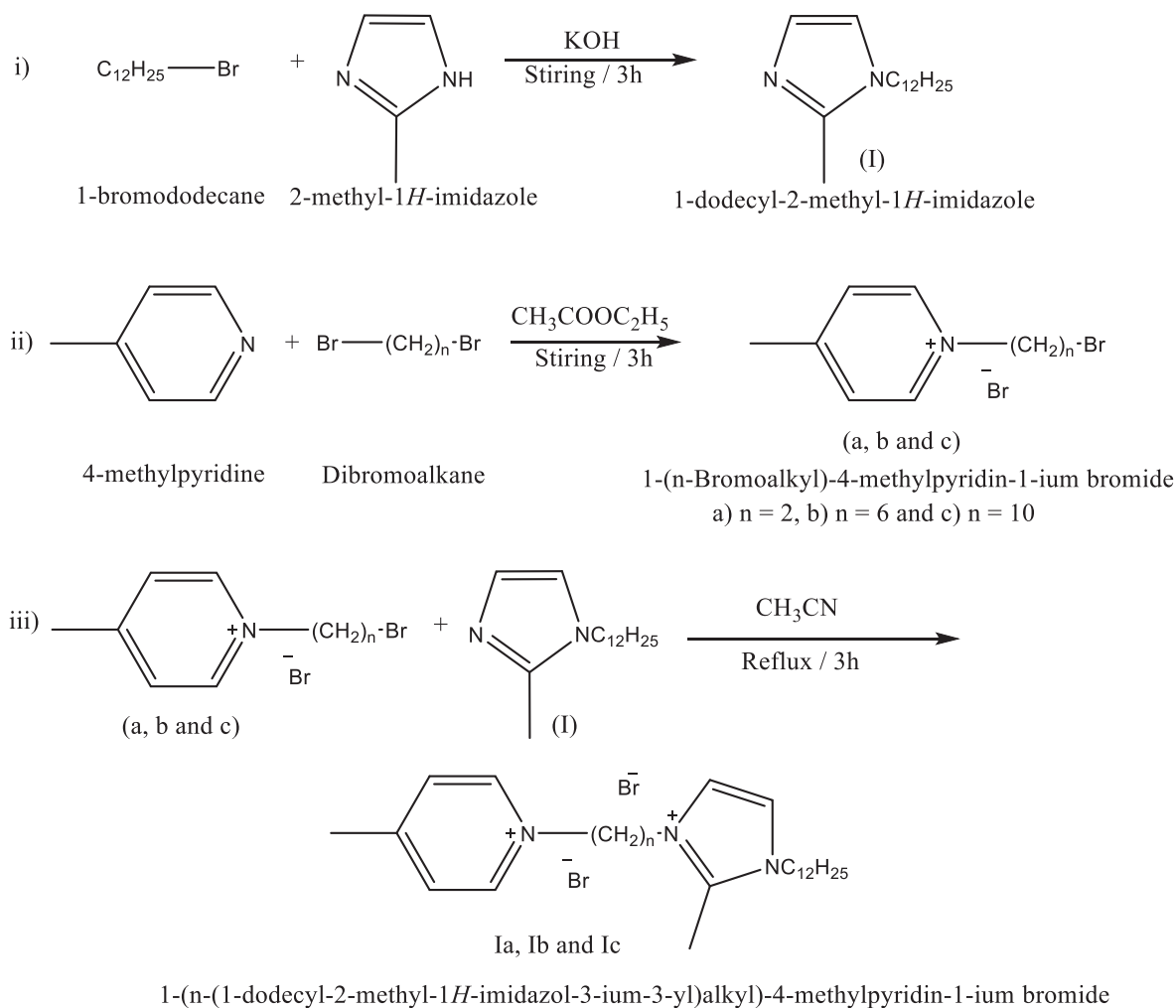
- Elemental Analysis: Elemental analysis was performed via elemental analyzer Perkin Elmer 240C.
- FT-IR Spectroscopy: FT-IR spectra were obtained from Nicolet Ia-10 in the range of 4000–400 cm^{-1} with suitable scan resolution 4 cm^{-1} and scan rate 32 $\text{cm}^{-1}/\text{min}$.
- ^1H NMR Spectroscopy: ^1H NMR spectra for the prepared materials were obtained using BRUKER ^1H NMR spectroscopy. The spectrometer operates at 400.19 MHz and used 5-mm broad band inverse Z-gradient probe in $\text{DMSO } d_6$ solvent.
- Thermo-gravimetric Analysis (TGA): TGA analysis was achieved by simultaneous TGA-DSC (model: SDT Q600, USA) (EPRI).

2.3. Surface tension measurements of (Ia – c)

Surface tension measurements were carried out using a Du Nouy tensiometer with a platinum ring. Freshly prepared

Table 1 Names and chemical structures of the synthesized compounds.

Compound	Chemical name	Chemical structure
Ia	1-(2-(1-dodecyl-2-methyl-1 <i>H</i> -imidazol-3-ium-3-yl)ethyl)-4-methylpyridin-1-ium bromide	
Ib	1-(6-(1-dodecyl-2-methyl-1 <i>H</i> -imidazol-3-ium-3-yl)hexyl)-4-methylpyridin-1-ium bromide	
Ic	1-(10-(1-dodecyl-2-methyl-1 <i>H</i> -imidazol-3-ium-3-yl) decyl)-4-methylpyridin-1-ium bromide	



Scheme 1 Synthesis of dicationic ionic liquids (Ia, Ib & Ic).

aqueous solutions of asymmetric dicationic ILs were measured over a concentration range of 0.01–0.00001 M/L at 25 °C. The surface tension of double distilled water was measured to calibrate instruments, which was generally 72.00 ± 0.50 mN/m (El-Dib et al., 2013; Nessim et al., 2018).

Interfacial tension measurements using paraffin oil at 25 °C. Emulsion stability was measured by vigorously stirring a mixture of 10 ml (0.5%) of solution and 10 ml of paraffin oil at 25 °C (Abdallah et al., 2007).

2.4. Physicochemical properties of the delivered crude oil

Physicochemical characteristics of the crude oil sample were studied according to standard methods (water content (ASTM D-95), pour point (ASTM D-97), viscosity & viscosity index (ASTM D-445), density (ASTM D-4052), flash point (ASTM D-93), asphaltene content (IP 43) and wax content (UOP 64)).

2.5. Evaluation of (Ia – c) as oil spill dispersants

2.5.1. Efficiency test

Studying the efficiency of the prepared ILs as oil spill dispersants at different temperatures and concentration as following (Deyab et al., 2020):

- A definite amount of sea water sample (250 ml) is transferred to a separating funnel and maintained at required temperature and then (5 ml) of used crude oil was added to the water surface and left for 1 min.
- A known amount of dispersant was added. After a time of 2.5 min from the addition of oil, the oil was shaken for two minutes, then 50 ml of the oily water was drawn in a 50 ml measuring cylinder in a time not exceeding 10 s. Then, the oily water was transferred from the measuring cylinder to separating funnel.
- The measuring cylinder was washed twice with 10 ml of chloroform. The washing was added to separating funnel, and shaken for 1 min. Two phases were allowed to separate completely and run off the chloroform layer through a Whatman filter paper No.1 containing anhydrous sodium sulphate. Chloroform extraction was repeated twice more using 20 ml of chloroform. The dried extracts and washings were combined in 100 ml volumetric flask to mark, stopped and mixed well.
- Calibration, of used crude oil is made at different concentrations (0.1, 0.2, 0.3, 0.4 & 0.5 g) in chloroform. The absorbance of each solution is measured at 580 nm. Fig. 1.

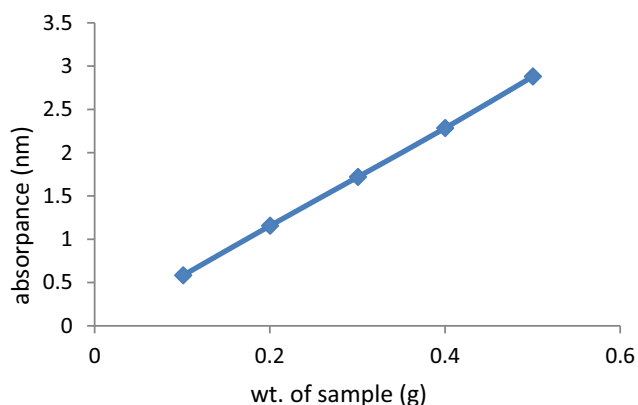


Fig. 1 Calibration curve.

- The absorption of the chloroform extract was measured against a chloroform blank at 580 nm in glass cells of 5 mm path length. Using calibration curve the weight of oil, contained in the 50 ml oily water sample was calculated.

The efficiency index E, was calculated from the equation

$$E\% = \text{Weight of oil in 50 ml sample of oily water} \times 500 / \text{total weight of added oil to 250 ml.}$$

3. Results & Discussions

3.1. Characterization of (Ia-c)

3.1.1. Elemental analysis

Data obtained from Table 2 showed that the observed values of the synthesized ionic liquids are in good compatibility with the calculated ones.

3.1.2. FT-IR Spectroscopy

Fig. 2 and Table 3 reveals the presence of characteristic bands of the synthesized Ia-c matched with their proposed structures.

N.B: Bands appeared at 3440–3416 cm^{-1} (Ia), 3422 cm^{-1} (Ib) and 3405 cm^{-1} (Ic) assigned to stretching vibrations bands of hydrogen bonded H_2O molecules (Brycki et al., 2017; Mohamed et al., 2017).

3.1.3. ^1H NMR Spectroscopy:

^1H NMR data recorded from Fig. 3 and Table 4 were in good compatibility with the chemical structures of Ia-c.

3.1.4. Thermo-gravimetric analysis (TGA)

Fig. 4 illustrated the degradation onset temperature which showed endurance of (Ia-c) against temperature. It can be cleared that (Ia-c) have high thermal stability and the decomposition started at 220, 255 and 265 $^{\circ}\text{C}$ respectively. This is what distinguishes ionic liquids. It was noticed that the longer alkyl chain spacer, the higher thermal stability (Jiangou et al., 2020; Zahoor Ullah et al., 2015; Zahoor Ullah et al., 2016).

3.2. Surface tension measurements

3.2.1. Emulsification power and interfacial tension

Table 5 listed the emulsification tendency of Ia-c in presence of light paraffin oil. It is clear that emulsification power is completely dependent on space chain length. Increasing hydrophobic chain length decreased the stability of oil-in-water (o/w) emulsion (Zeng et al., 2018).

On the other hand, the interfacial tension is related to the saturation of the surface-active ionic liquid molecules at the interface. Data in Table 6 revealed that the interfacial tension of Ia-c is decreased by increasing the spacer chain length, and the lowest interfacial tension was obtained in presence of the longest spacer chain of this series.

3.2.2. Surface parameters

Surface tension and critical micelle concentration:

Surface tension was investigated to evaluate the surface activity of Ia-c in aqueous solution at the ambient temperature. As illustrated in Fig. 5, the surface tension slowly decreased with increasing concentration for Ia-c, suggesting that the molecules of Ia-c appeared to adsorb at air–water interface. Then, a plateau was obtained in (γ -log C) plot, which implies that adsorption saturation and aggregates are produced. These plots's breakpoints correspond to the concentration of critical aggregation (CMC). Values of CMC and the surface tension at CMC (γ CMC) for all three synthesized ionic liquids are listed in Table 5. It was evident that Ia-c were have superior surface activities.

Ia-c showed unique self-assembly behaviour in water. It is apparent that increasing the length of connecting linkage chain slightly decreases the surface tension. At room temperature, Ia-c show sharp breaks of the surface tension vs $-\log$ (concentration) isotherm, indicating critical concentration of micellization (cmc) and micellular formation. Results reveals that Ia-c have low cmc and high efficacy in reducing surface tension of water, Ib has the lowest value.

When the length of hydrophobic spacer increased, flexible methylene chain will become part of the micelle hydrophobic

Table 2 Elemental analysis of Ia-c.

Comp.	Elements							
	C%		H%		N%		Br %	
	Calc.	Obs.	Calc.	Obs.	Calc.	Obs.	Calc.	Obs.
Ia	54.24	54.31	7.78	7.72	7.91	7.85	30.07	30.12
Ib	57.24	57.03	8.41	8.54	7.15	7.26	27.20	27.17
Ic	59.72	59.67	8.93	8.85	6.53	6.61	24.83	24.87

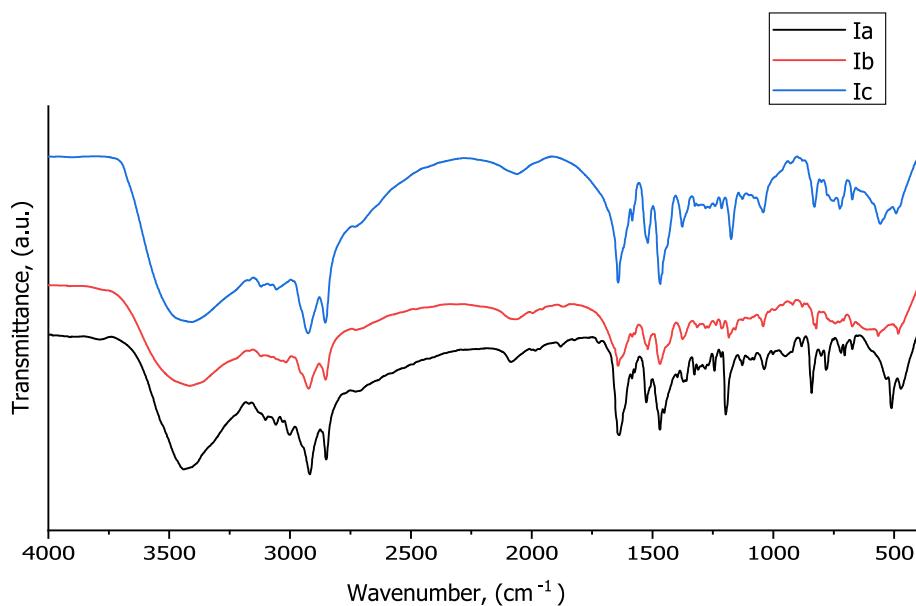


Fig. 2 FT-IR Spectroscopy of Ia-c.

Comp.	$\nu \text{ cm}^{-1}$					
	CH-H ₂ O	C-H aromatic	C-H aliphatic	N-H Combination	C=C C=N	C-C
Ia	3440	3001 3058 3101	2850 2918	2085	1637	1525
Ib	3416	3017	2922 2858	2068	1642	1519
Ic	3405	3056 3120	2925 2854	2061	1641	1519

core, it can reduce free energy, resulting in a lower CMC value (Pisářík et al., 2016; Pal et al., 2017).

Effectiveness (π_{CMC}):

The difference between the surface tension of Ia-c at their CMC and that of pure water is termed “effectiveness” (π_{CMC}):

$$\pi_{\text{CMC}} = \gamma_0 - \gamma$$

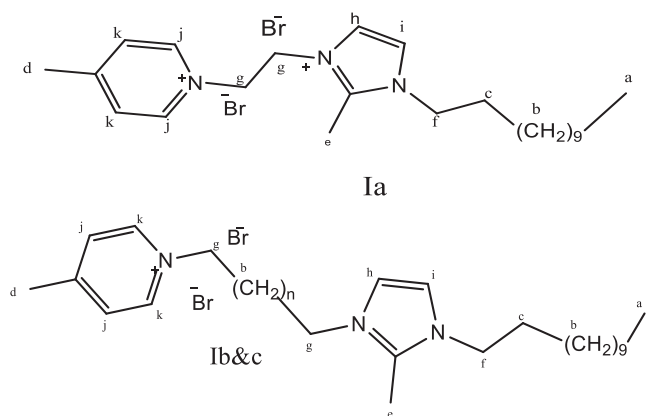


Fig. 3 ¹H NMR structures of (Ia-c).

where γ_0 is the surface tension of the pure water and γ is the surface tension of the surfactant solution at CMC (Negm and Mohamed, 2004).

The effectiveness of Ia-c ranged between 38 and 40 dyn/cm at 25 °C (Table 5). It is obvious that Ia-c are efficient in achieving the maximum reduction of surface tension at cm, Table 5.

ii. Efficiency (P_{C20})

For Ia-c, the P_{C20} -values were determined Table 5. These values commonly characterize the efficiency of them to lower surface tension.

Values of C20 for Ia-c indicate that they have great efficiency in reducing surface tension of water and showed high surface activity.

iii. Maximum surface excess (Γ_{max})

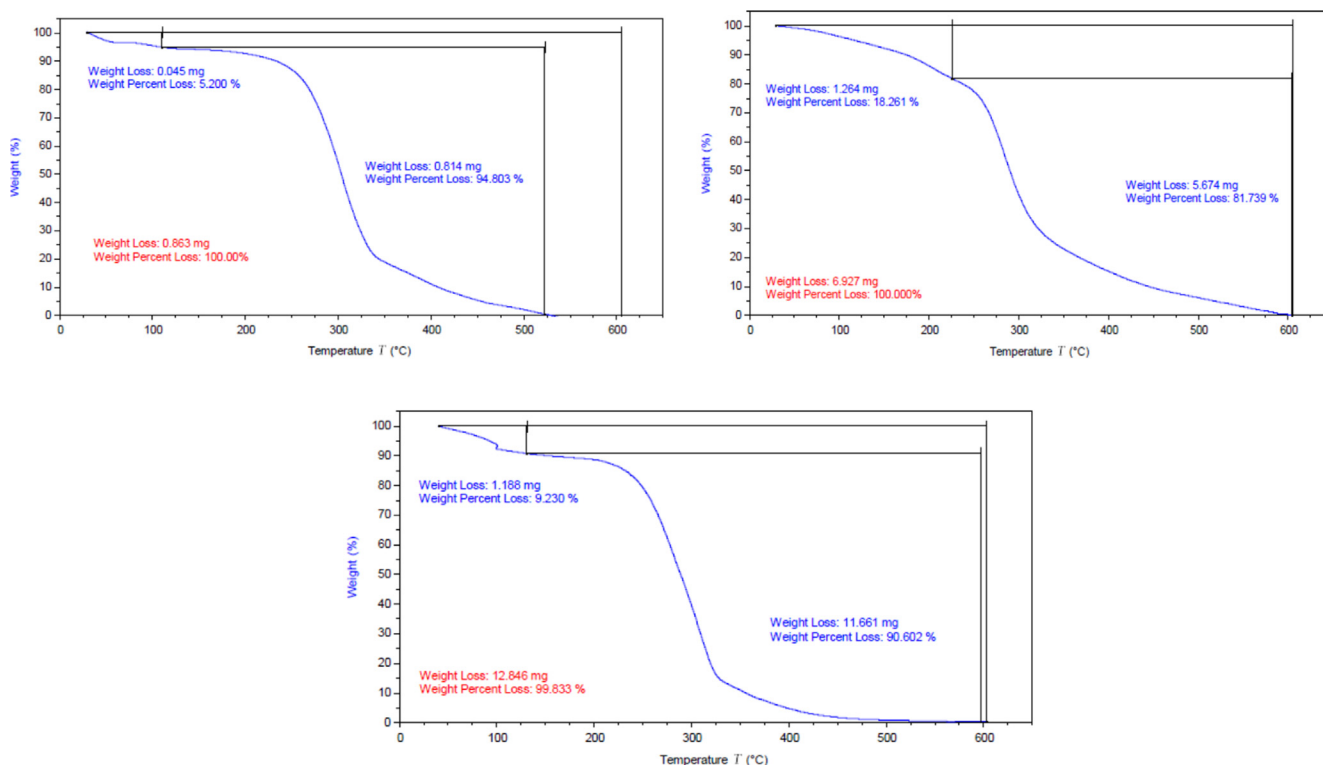
Γ_{max} can be calculated according to the Gibbs equation:

$$\Gamma_{\text{max}} = -(\delta\gamma/\delta\log c)_T / 2.303nRT,$$

where Γ_{max} is the surface excess, $d\gamma$ is the surface pressure, and C is the concentration of ionic liquids. Values of Γ_{max} are

Table 4 ^1H NMR spectroscopy.

Chemical shift (δ ppm)											
Comp.	a (t)	b (t)	c (m)	d (s)	e (s)	f (t)	g (t)	h (d)	i (d)	j (d)	K (d)
Ia	0.86	1.24	1.73	2.51	2.63	4.09	5.21	7.71	8.04	8.90	9.14
Ib	0.86	1.29	1.72	2.51	2.63	4.04	4.56	7.74	7.99	8.01	9.01
Ic	0.84	1.23	1.72	2.51	2.62	4.10	4.57	7.59	7.69	8.01	9.00

**Fig. 4** TGA for Ia-c.**Table 5** Surface parameters of the synthesized ILs (Ia-c).

ILs	CMC mol./L	γ_{CMC} mN/m	π_{CMC} mN/m	Pc_{20}	$\Gamma_{\text{max}} \times 10^{11}$ mol./cm 2	A_{min} nm 2	$\Delta G_{\text{mic}}^{\circ}$ KJ/mol	$\Delta G_{\text{ads}}^{\circ}$ KJ/mol
Ia	5×10^{-3}	34	38	5×10^{-6}	3.51	47.301	-13.129	-23.955
Ib	1.6×10^{-3}	32	40	2.5×10^{-6}	4.286	38.738	-15.953	-23.886
Ic	7.5×10^{-3}	33	39	2.5×10^{-5}	3.974	41.78	-12.125	-21.184

Table 6 Surface properties of the synthesized surfactants (Ia-c).

Surfactants	IFT mN/m	Emulsification s
Ia	9	165
Ib	5	110
Ic	4	49

showed in **Table 5** indicate that with positive Γ_{max} surface tension decreased with increasing ionic liquids activity.

Changing the length of the spacer at the aqueous solution/air interface seemed to have very little effect on their effectiveness.

iv. Minimum surface area (A_{min})

The minimum surface area (A_{min}) can be calculated from the following equation:

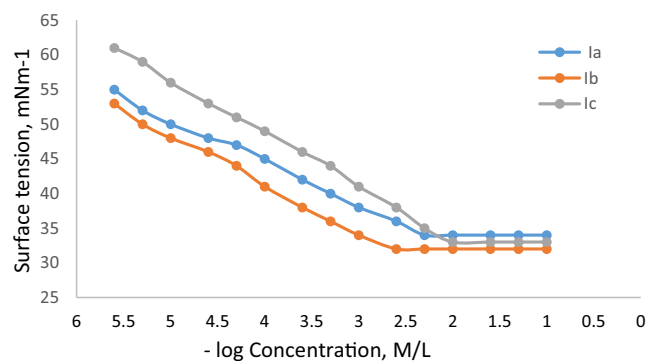


Fig. 5 Surface tension isotherm of Ia-c at 25 °C.

Table 7 Physicochemical characterization of crude oil.

Experiment	Method	Result
Density@ 15.56 °C	ASTM D-4052	0.9558
Specific gravity		0.8568
API gravity@15.56 °C		16.3
Kinematic Viscosity @40 °C, cSt	ASTM D-445	1820.35
Asphaltene content, wt%	IP-143	13.35
Wax content, wt%	UOP-64	1.37
Water content, vol%	ASTM D-97	7.5
Pour point, °C	ASTM D-95	15
Flash point, °C	ASTM D-93	< -22

$$A_{min} = 10^{16} / N \cdot \Gamma_{max}$$

where N is Avogadro's number. A_{min} values decreased with an increase in length of spacer. This indicates that the molecules for the longer-chain alkyl surfactants were more tightly packed at the air / water interface. The saturation surface excess concentration (Γ_{max}) increases as A_{min} decreases (Nakahara et al., 2019).

Standard free energy of micellization (ΔG_{mic}°), and standard free energy of adsorption (ΔG_{ads}°):

ΔG_{mic}° can be calculated from the following equation:

$$\Delta G_{mic}^{\circ} = RT \ln CMC$$

ΔG_{mic}° for Ia-c were always negative values, indicating that micellization was a spontaneous process. The general trend of $-\Delta G_{mic}^{\circ}$ increase with increasing the distance between the two heads groups (spacer), i.e., it became less negative. This indicates that increasing in the spacer length, hydrophobicity, favor the micellization process.

Conversely, ΔG_{ads}° can be calculated by the relation

$$\Delta G_{ads}^{\circ} = \Delta G_{mic}^{\circ} - (0.6xp_{cmc} \cdot xA_{min})$$

Table 5 showed some increase in ΔG_{ads}° , supporting the idea of micellization over adsorption on the solution surface to overcome the repulsion forces occurring at the water/hydrophobe interface. ΔG_{ads}° and ΔG_{mic}° were always negative in value due to the spontaneity, and indicating that the processes are thermodynamically favoured (Ahmed et al., 2018).

3.3. Physicochemical properties of crude oil

The studied crude oil was heavy as shown from Table 7.

Table 8 Efficiency of Ia-c. Ia.

Ia	Concentrations, ppm			
	750	1500	2000	3000
Temp. °C				
	Efficiency, %			
10	3.04	16.51	12.48	8.21
30	12.64	48.71	45.99	43.33
50	19.15	52.84	50.98	49.26
Ib.				
	Concentration, ppm			
Temp. °C	750	1500	2000	3000
	Efficiency, %			
10	13.47	33.61	23.61	11.57
30	21.90	66.80	61.08	54.32
50	32.69	75.50	70.62	55.22
Ic.				
	Concentration, ppm			
Temp. °C	750	1500	2000	3000
	Efficiency, %			
10	9.25	12.66	10.95	2.68
30	28.34	36.98	31.24	29.97
50	41.60	51.22	48.73	36.98

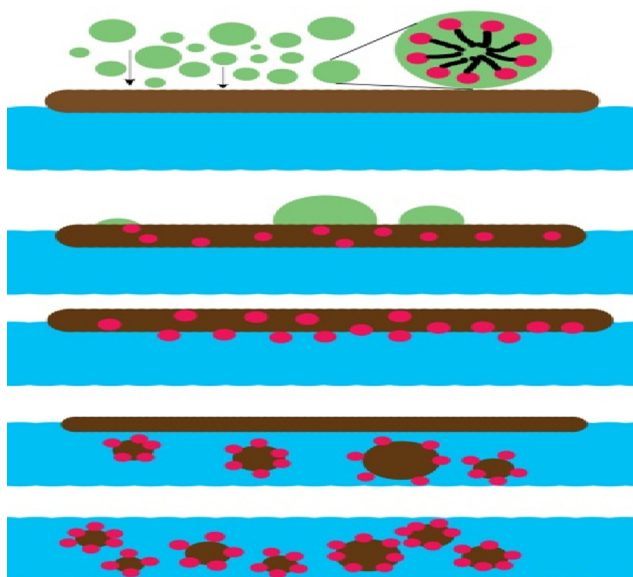


Fig. 6 The dispersion mechanism.

3.4. Evaluation of (Ia-c) as oil spill dispersants:

Tables 8–10 showed that the dispersion efficiency increased with increasing concentration from 750 to 1500 ppm and started slightly decreased at 2000 ppm for the three compounds. By using 3000 ppm, there was no change in efficiency of them occurred. It was noticed that the efficiency increased with increasing temperature.

Table 8 illustrated the follows:

- The amphiphilic synthesized ionic liquids might be absorbed compactly at the oil droplet surfaces to form the

emulsion which is sun like structure. Also, the non-polar ends of Ia, Ib & Ic would form stable emulsion structure through van der waals forces (Shi, 2020; Jin et al., 2018) when the size of crude oil decrease and form a spring like structure (Fig. 6).

- Ia, with the shortest spacer, makes the two cations very close so the effect of alkyl chain could be neglected. The dispersion efficiency of Ia at the optimum concentration (1500 ppm) start from 16.51% at 10 °C to 52.84% at 50 °C.
- On the other hand, Ib with six carbon atoms spacer the two aromatic cations became far apart. So, the effect of lyophobic part increased and the dispersion efficiency increased at 1500 ppm to reach to 33.61 at 10 °C and 75.50 at 50 °C.
- In case of Ic which has the longest spacer (ten carbon atoms) the spacer alkyl chain increased but there are another factors affected, i) the steric bulk twisted therefore the characters differ, and ii) the hydrophobic interaction become more strong due to the longest spacer chain and prevent the emulsion stability (Jin et al., 2018; Huang et al., 2019; Ismail et al., 2020) as shown in Fig. 7. Ic possess the least efficiency which start from 12.66% at 10 °C to 51.22 at 50 °C for 1500 ppm as concentration.

4. Conclusion

From the previous study we concluded the following

- New series of environmentally asymmetric dicationic ionic liquids (Ia-c) were prepared and successfully well characterized.
- They were studied as surface active compounds.
- They were evaluated as oil spill dispersants in sea water (Red Sea).
- The three compounds possessed high efficiency.
- The efficiency is ranked as follows: Ib > Ia > Ic with the concentration of 1500 ppm.

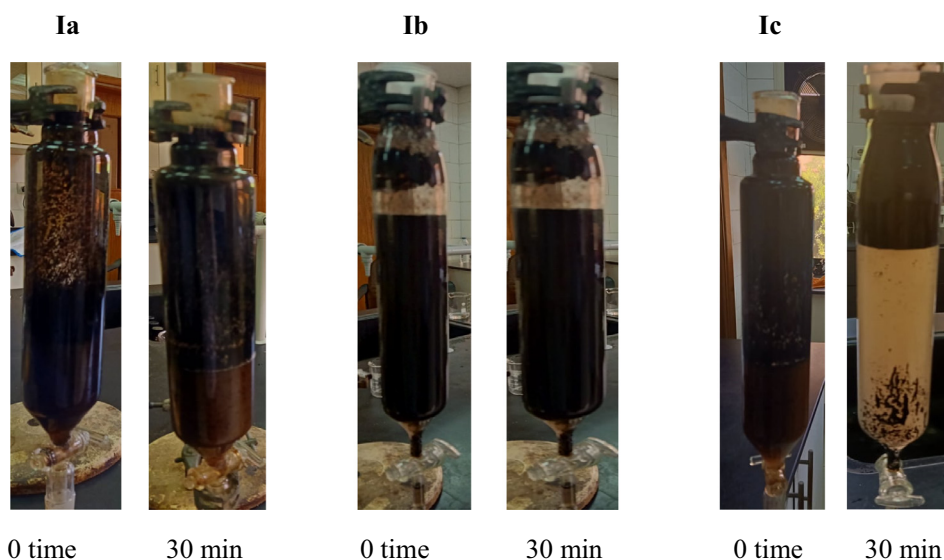


Fig. 7 Photos of petroleum crude oil water emulsions in the presence of IL at 0 time and after 30 min for 1500 ppm.

Declaration of Competing Interest

The authors declare that they have no known competing financial interests or personal relationships that could have appeared to influence the work reported in this paper.

References

- Abdallah, R.I., Mohamed, S.Z., Ahmed, F.M., 2007. Effect of biological and chemical dispersants on Oil spills. *Petrol. Sci. Technol.* 23, 463–474.
- Abdullah, Mahmood M.S., AlQuraishi, Abdulrahman A., Allohedan, Hamad A., AlMansour, Abdullah O., Atta, Ayman M., 2017. Synthesis of novel water soluble poly (ionic liquids) based on quaternary ammonium acrylamidomethyl propane sulfonate for enhanced oil recovery. *J. Mol. Liq.* 233, 508–516.
- Adawiyah, N.M., Hawatulaila, S.B., Atikah, A.A., Vijaya Bhaskar Reddy, A., Mutalib, M.I.A., Moniruzzaman, M., 2019. Synthesis, characterization, ecotoxicity and biodegradability evaluations of novel biocompatible surface active lauroyl sarcosinate ionic liquids. *Chemosphere* 447, 349–357.
- Adeniyi Ogunlaja, S., Olalekan, S., Alade, 2018. Catalysed oxidation of quinoline in model fuel and the selective extraction of quinoline-N-oxide with imidazoline-based ionic liquids. *Egypt. J. Petrol.* 27, 159–168.
- Ahmed, S.M., Khidr, T.T., Ismail, D.A., 2018. Effect of gemini surfactant additives on pour point depressant of crude oil. *J. Disp. Sci. Technol.* 39, 1160–1164.
- Atta, A.M., Ezzat, A.O., Abdullah, M.M., Hashem, A.I., 2017. Effect of different families of hydrophobic anions of imidazolium ionic liquids on asphaltene dispersants in heavy crude oil. *Energy Fuels* 31, 8045–8053.
- Atta, A.M., Abdullah, M.M., Al-Lohedan, H.A., Gaffer, A.K., 2018. Synthesis and application of amphiphilic poly (ionic liquid) dendron from cashew nut shell oil as a green oilfield chemical for heavy petroleum crude oil emulsion. *Energy Fuels* 32, 4873–4884.
- Behera, S.S., Ray, R.C., 2016. Konjac glucomannan, a promising polysaccharide of *Amorphophallus konjac* K. Koch in health care. *Int. J. Biol. Macromol.* 92, 942–956.
- Brycki, B., Meteka, I., Kozirog, A., Otlewska, A., 2017. Synthesis, structure and antimicrobial properties of novel benzalkoniumchloride analogues with pyridine rings. *Molecules* 22, 130.
- Chang, Jui-Cheng, Ho, Wen-Yueh, Sun, I-Wen, Yung-LiangTung, Meng-Chin Tsui, Tzi-Yi, Wu, Liang, Shih-Shin, 2010. Synthesis and characterization of dicationic ionic liquids that contain both hydrophilic and hydrophobic anions. *Tetrahedron* 66, 6150–6155.
- Deyab, M.A., Moustafa, Y.M., Nessim, M.I., Fathallah, Nesreen A., Asaad Bagato, Noha M., 2020. Asaad Bagato, New series of ionic liquids based on benzalkonium chloride derivatives: Synthesis, characterizations, and applications. *J. Mol. Liquids* 313, 113566. <https://doi.org/10.1016/j.molliq.2020.113566>.
- El-Dib, F.I., Ahmed, S.M., Ismail, Dina A, Mohamed, D.E., 2013. Synthesis and Surface Properties of Novel N-Alkyl Quinoline-Based Cationic Gemini Surfactants. *J. Disp. Sci. Technol.* 34, 596–603.
- El-Nagar, R.A., Nessim, M., Abd El-Wahab, A., Ibrahim, R., Faramawy, S., 2017. Investigating the efficiency of newly prepared imidazolium ionic liquids for carbon dioxide removal from natural gas. *Journal of Molecular Liquids* 237, 484–489.
- El-Taib Heakal, F., Deyab, M.A., Osman, M.M., Nessim, M.I., Elkholy, A.E., 2017. Synthesis and assessment of new cationic Gemini surfactants as inhibitors for carbon steel corrosion in oilfield water. *RSC Adv.* 7, 47335–47352.
- Ezzat, A.O., Atta, A.M., Al-Lohedan, H.A., Abdullah, M.M., Hashem, A.I., 2018. Synthesis and application of poly (ionic liquid) based on cardanol as demulsifier for heavy crude oil water emulsions. *Energy Fuels* 32, 214–225.
- Huang, D., Sebastian, R., Zhang, L., Hongfei, X.u., Lei, S., Chen, M., Shinde, A., Ma, Rong, Sam Mannan, M., Cheng, Zhengdong, 2019. Biocompatible Herder for rapid oil spill treatment over a wide temperature Range. *J. Loss Prev. Process Ind.* 62, 103948.
- Huanga, D., Sebastian, R., Zhange, L., Xub, H., Leic, Sh., Chenc, M., Shinde, A., Mac, R., Mannan, M.S., Cheng, Zh., 2019. Biocompatible Herder for rapid oil spill treatment over a wide temperature Range. *J. Loss Prev. Process Ind.* 62, 103948.
- Ismail, A.I., Atta, A.M., El-Newehy, M., El-Hefnawy, M.E., 2020. *Polymers* 12, 1273.
- Jiangou, Yu, Wheelhouse, Richard T., Honey, Mark A., Karodia, Nazira, 2020. *J. Mol. Liquids* 316, 113857.
- Jin, J., Wang, H., Jing, Y., Liu, M., Wang, D., Li, Y., Bao, M., 2018. An Efficient and environmental-friendly dispersant based on the synergy of amphiphilic surfactants for oil spill remediation. *Chemosphere* 215, 241–247.
- Komoto, I., Kobayashi, S., 2004. Lewis acid catalysis in supercritical carbon dioxide. Use of poly (ethylene glycol) derivatives and perfluoroalkylbenzenes as surfactant molecules which enable efficient catalysis in ScCO₂. *J. Org. Chem.* 69 (3), 680–688.
- Kujawinski, E.B., Kido Soule, M.C., Valentine, D.L., Boysen, A.K., Longnecker, K., Redmond, M.C., 2011. Fate of dispersants associated with the deepwater horizon oil spill. *Environ. Sci. Technol.* 45 (4), 1298–1306.
- Li, Zhonghao, Jia, Zhen, Luan, Yuxia, Mu, Tiancheng, 2008. Ionic liquids for synthesis of inorganic nanomaterials. *Curr. Opin. Solid State Mater. Sci.* 12 (1), 1–8.
- Li, Z.H., Luan, Y.X., Mu, T.C., 2009. Unusual nanostructured ZnO particles from an ionic liquid precursor. *Chem. Commun.* 10, 1258–1260.
- Lotfi, M., Moniruzzaman, M., Sivapragasam, M., Kandasamy, S., Mutalib, M.I.A., Noorjahan, B.A., Goto, M., 2017. Solubility of acyclovir in nontoxic and biodegradable ionic liquids: COSMO-RS prediction and experimental verification. *J. Mol. Liq.* 243, 124–131.
- Ly, Wei-Feng, Zhou, Zhao-Hui, Zhang, Qun, Luo, Wen-Li, Wang, Hong-Zhuang, Ma, De-Sheng, Zhang, Lei, Wang, Rong, Zhang, Lu, 2019. Wetting of polymer surfaces by aqueous solutions of branched cationic Gemini surfactants. *Soft Matter* 15, 6725–6731.
- Mohamed, A.I.A., Sultan, A.S., Hussein, I.A., Al-Muntasheri, G.A., 2017. Influence of Surfactant Structure on the Stability of Water-in-Oil Emulsions under High-Temperature High-Salinity Conditions. *J. Chem.* 1, 11.
- Muhd Julkapli, N., Akil, H.M., Ahmad, Z., 2011. Preparation, properties and applications of chitosan-based biocomposites/blend materials: a review. *Compos. Interfac.* 18, 449–507.
- Nakahara, H., Nishino, A., Tanaka, A., Fujita, Y., Shibata, O., 2019. Interfacial behavior of gemini surfactants with different spacer lengths in aqueous medium. *Colloid Polym. Sci.* 297, 183–189.
- Naser, H.A., 2013. Assessment and management of heavy metal pollution in the marine environment of the Arabian Gulf: A review. *Mar. Pollut. Bull.* 72 (1), 6–13.
- Negm, Nabel A., Mohamed, Ammona S., 2004. Surface and Thermodynamic Properties of Diquaternary Bola-Form Amphiphiles Containing an Aromatic Spacer. *J. Surf. Deterg.* 7 (1), 23–30.
- Nessim, M.I., Osman, M.M., Ismail, D.A., 2018. Surface-active properties of new cationic gemini surfactants with cyclic spacer. *J. Disp. Sci. Technol.* 39, 1047–1055.
- Pal, N., Saxena, N., Mandal, A., 2017. Synthesis, characterization, and physicochemical properties of a series of quaternary gemini surfactants with different spacer lengths. *Colloid Polym. Sci.* 295, 2261–2277.
- Pandey, Siddharth, 2006. Analytical applications of room-temperature ionic liquids: a review of recent efforts. *Anal. Chim. Acta* 556 (1), 38–45.
- Penela-Arenaz, M., Bellas, J., Vázquez, E., 2009. Chapter five: effects of the prestige oil spill on the biota of NW Spain: 5 years of learning. *Adv. Mar. Biol.* 56, 365–396.

- Pisárcik, M., Jampilek, J., Devinsky, F., Drábiková, J., Tkacz, J., Opravil, T., 2016. Gemini Surfactants with Polymethylene Spacer: Supramolecular Structures at Solid Surface and Aggregation in Aqueous Solution. *J. Surfact. Deterg.* 19, 477–486.
- Shi, Baoli, 2020. The strengths of van der Waals and electrostatic forces in 1-alkyl-3-methylimidazolium ionic liquids obtained through Lifshitz theory and Coulomb formula. *J. Mol. Liquids* 320, 114412. <https://doi.org/10.1016/j.molliq.2020.114412>.
- Visser, Ann E., Swatloski, Richard P., Reichert, W. Matthew, Davis Jr., James H., Rogers, Robin D., Mayton, Rebecca, Sheff, Sean, Wierzbicki, Andrzej, 2011. Task-specific ionic liquids for the extraction of metal ions from aqueous solutions. *Chem. Commun.* (1), 135–136 <https://doi.org/10.1039/b008041l>.
- Wilkes, John S., 2002. A short history of ionic liquids – from molten salts to neoteric solvents. *Green Chem* 4 (2), 73–80.
- Zahoor Ullah, M., Bustam, Azmi, Man, Zakaria, Muhammad, Nawshad, Khan, Amir Sada, 2015. Synthesis, characterization and the effect of temperature on different physicochemical properties of protic ionic liquids. *RSC Advances* 87.
- Zahoor Ullah, M., Bustam, Azmi, Man, Zakaria, Khan, Amir Sada, 2016. Thermal stability and kinetic study of benzimidazolium based ionic liquid. *Proc. Eng.* 148, 215–222.
- Zeng, X., Zhang, Y., Li, Y., Wang, W., Wang, L., 2018. Synthesis and solution properties of ionic liquid type polysiloxane bola surfactants. *J. Disp. Sci. Technol.* 39, 227–233.